

A tunable low-drift laser stabilized to an atomic reference

T. Leopold¹, L. Schmöger^{1,2}, S. Feuchtenbeiner², C. Grebing¹, P. Micke^{1,2}, N. Scharnhorst¹, I.D. Leroux¹, J.R. Crespo López-Urrutia², P.O. Schmidt^{1,3}

¹ Physikalisch-Technische Bundesanstalt, 38116 Braunschweig, Germany

² Max-Planck-Institut für Kernphysik, 69117 Heidelberg, Germany

³ Institut für Quantenoptik, Leibniz Universität Hannover, 30167 Hannover, Germany

Received: date / Revised version: date

Abstract We present a laser system with a linewidth and long-term frequency stability at the 50 kHz level. It is based on a Ti:Sapphire laser emitting radiation at 882 nm which is referenced to an atomic transition. For this, the length of an evacuated transfer cavity is stabilized to a reference laser at 780 nm locked to the ^{85}Rb D₂-line via modulation transfer spectroscopy. Full tunability of the spectroscopy laser is realized using the sideband locking technique to the transfer cavity. In this configuration, the linewidth of the spectroscopy laser is derived from the transfer cavity, while the long-term stability is derived from the atomic resonance. The frequency stability and linewidth of both lasers are characterized by comparison against an active hydrogen maser frequency standard and an ultra-narrow linewidth laser, respectively. The spectral gaps are bridged with an optical frequency comb. The laser system presented here will be used for spectroscopy of the $1s^2 2s^2 2p$ $^2P_{1/2}$ – $^2P_{3/2}$ transition in sympathetically cooled Ar^{13+} ions at 441 nm after frequency doubling.

1 Introduction

Laser spectroscopy is a powerful tool to gain insight into the structure of atoms and molecules. The development of laser cooling and trapping techniques has enabled precision spectroscopy of atoms and ions, culminating in the realization of high accuracy optical clocks [1–4]. Repeated comparisons between frequency standards allows to study a possible change in fundamental constants [5–7]. Highly charged ions (HCIs) are particularly interesting for such tests of fundamental physics and have potential for superior optical clocks. Due to high relativistic contributions to the binding energy of their electrons, some transitions in HCIs are exceptionally sensitive to a change of the fine structure constant [8].

Also, small polarisabilities and high internal fields render HCIs insensitive to external perturbations, promising small systematic shifts in atomic clocks based on optical transitions in HCIs [9, 10]. However, laser spectroscopy of HCIs is still in its infancy. The highest resolution in laser spectroscopy of HCIs has been demonstrated on the dipole forbidden $^2P_{1/2}$ to $^2P_{3/2}$ transition in Ar^{13+} with a pulsed dye laser, reaching a resolution of ~ 400 MHz [11]. This measurement was limited by the large kinetic energy of the HCIs in the electron beam ion trap. Sympathetic cooling to the mK regime by embedding the Ar^{13+} ions in a laser cooled crystal of Be^+ ions [12] reduces this limitation. In the current setup resolutions on the order of 100 kHz of this line with an excited state lifetime of 10 ms [11] can be expected. Such a measurement requires a continuous-wave spectroscopy laser with a linewidth and long-term drift below 100 kHz. There are several ways to achieve this goal. The spectroscopy laser can be locked to a passive cavity [13–15], to a stabilized optical frequency comb [16–20] or to a broad atomic or molecular transition either directly [21–26] or via a transfer cavity [27]. In our specific case, the laser will be transported from PTB in Braunschweig, where it is built and calibrated to the MPIK in Heidelberg, where the HCI spectroscopy will be performed. While stabilization to a passive cavity can in principle provide the required performance goals, a significant engineering effort is required to make it transportable [28–31]. Furthermore, cavities exhibit long-term drifts of their resonances that are not predictable [32]. For decades, lasers have been stabilized to atomic references that can in principle provide light with very small long-term drift. However, typically two issues have to be overcome: often there are no suitable atomic transitions close to the spectroscopy laser frequency, and the linewidth of the transition may be broader than required for the target laser linewidth. Both issues can be resolved using a frequency comb referenced to a stable cavity or atomic reference that allows to transfer the stability of the reference to the spectroscopy laser on all relevant

time scales [19, 20]. However, a comb and a suitable reference are required for such an approach, both of which are resource intensive and therefore not generally available in all laboratories.

As an alternative a cavity can be used to transfer the stability of a reference laser to the spectroscopy laser [27, 33–38]. To achieve simultaneous resonance of both lasers with the transfer cavity, at least one of them must be tunable by one free spectral range (FSR). For common cavity lengths the FSR is on the order of 1 GHz.

Here, we report on a setup to stabilize a spectroscopy laser with a wavelength of 882 nm via a transfer cavity to a reference laser operating at the Rb D₂-line wavelength of 780 nm. The reference laser is stabilized to the F=3 to F'=4 transition of the ⁸⁵Rb D₂-line using the modulation transfer spectroscopy technique [24, 26]. Frequency drifts of the atomic reference are suppressed by an active temperature stabilization of the Rb vapor cell and magnetic shielding. We use an evacuated cavity to transfer the reference laser's stability to the spectroscopy laser, thus avoiding environmental influences that affect the transfer lock's performance. The length of the cavity is actively stabilized to the reference laser frequency using the sideband locking technique in a Pound-Drever-Hall (PDH) setup [39]. The spectroscopy laser is then stabilized to the transfer cavity in a standard PDH configuration. Its frequency is widely tunable from 775 … 890 nm, limited by the coating range of the cavity mirrors. We operate at 882 nm to produce the spectroscopy wavelength of 441 nm for Ar¹³⁺ after frequency doubling.

By comparison with a maser using an optical frequency comb we show that the resulting frequency stability of the reference and spectroscopy laser is below 50 kHz on a timescale of several days. The short term linewidth is measured via a comparison with an ultra stable laser. Our setup enables us to narrow the linewidth of the spectroscopy laser to well below that of the reference laser, which reduces the requirements for the latter.

2 Experimental setup and results

The experimental setup is schematically shown in Fig. 1. It divides into three parts: the reference laser, the cavity transfer lock, and the spectroscopy laser, each of which will be discussed in detail in the following.

2.1 Reference laser

The reference laser consists of a distributed feedback laser diode (Eagleyard EYP-DFB-0780-00080) mounted in a temperature-stabilized housing (Thorlabs TCLDM9). A feedback signal can be applied via the low noise laser diode driver (Thorlabs LDC201CU, bandwidth 100 kHz) and a bias tee (bandwidth 500 MHz) permitting fast modulation of the diode pump current. The free running linewidth of the laser diode is specified

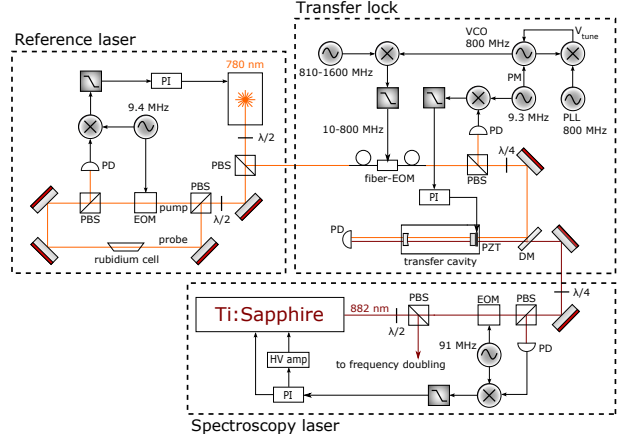


Fig. 1 Simplified experimental setup showing the reference laser, transfer lock setup and spectroscopy laser. For details about the individual parts of the setup refer to the corresponding sections. PBS: polarizing beam splitter, EOM: electro-optic modulator, PD: photo diode, DM: dichroic mirror, PZT: piezo actuator, PI: proportional-integral controller, VCO: voltage controlled oscillator, PLL: phase-locked loop, HV amp: high-voltage amplifier, PM: phase modulation, $\lambda/2$: half-wave plate, $\lambda/4$: quarter-wave plate, V_{tune} : mixer output/feedback voltage

to be around 2 MHz. The output power of ~ 50 mW is divided into two parts, 5 mW are used to stabilize the frequency to an atomic resonance by modulation transfer spectroscopy (MTS) [24, 26], the remainder is sent through a waveguide electro-optic modulator (EOM) towards the transfer cavity.

The optical setup for the frequency stabilization of the reference laser is shown in Fig. 1 in the upper left box. A linearly polarized pump beam, phase modulated at $\omega_{\text{MTS}} \simeq 9.4$ MHz, is aligned with an unmodulated probe beam in a temperature stabilized rubidium vapor cell. The rubidium vapor acts as a dispersive medium, which, detuned from resonance, converts the pump beam's phase modulation to amplitude modulation. The saturation of the medium is thus modulated with ω_{MTS} . The counterpropagating probe beam experiences a modulated absorption, which is subsequently detected as amplitude modulation on a photo diode. Homodyne mixing of the photo diode signal with ω_{MTS} yields a dispersion shaped output signal around the atomic resonance. This MTS signal is modified by a PI controller and fed back as a modulation of the current driving the laser diode.

In Fig. 2 the saturated absorption and MTS signals are shown when scanning the laser frequency around the D₂-line originating from the F=3 hyperfine ground state in ⁸⁵Rb and the F=2 ground state in ⁸⁷Rb [40, 41]. The advantages of the MTS technique for absolute frequency stabilization can be seen in the figure. Only the closed-cycle transitions F=3 to F'=4 in ⁸⁵Rb and F=2 to F'=3 in ⁸⁷Rb create a large error signal, resulting in a simple identification and reproducibility of the lock

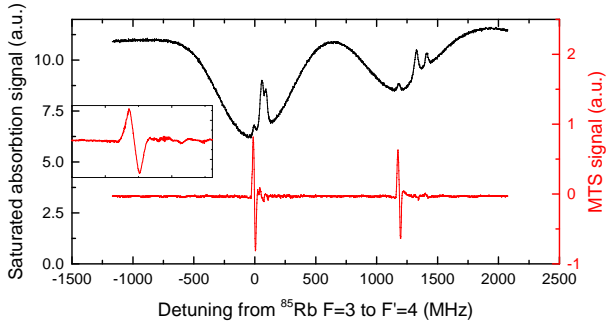


Fig. 2 The saturated absorption (black) and modulation transfer spectroscopy signal (red). Two Doppler broadened transitions contribute to the D₂-line for each isotope. Each consists of three hyperfine transitions. Here the transitions for ⁸⁵Rb F=3 to F'=2,3,4 and ⁸⁷Rb F=2 to F'=1,2,3 are shown. Only the cycling transitions F=3 to F'=4 (⁸⁵Rb) and F=2 to F'=3 (⁸⁷Rb) produce a strong dispersive signal in the modulation transfer spectroscopy. The inset shows a magnification of the ⁸⁵Rb transition used to stabilize the reference laser.

point. Furthermore, it exhibits a zero level DC background compared to frequency modulation or polarization spectroscopy [26]. However, a slight asymmetry of the error signal arises in MTS due to residual amplitude modulation (RAM) [42]. It has been shown that an absolute frequency accuracy below 1 kHz can in principle be achieved using MTS [43].

The vapor cell is temperature stabilized to ~ 10 mK root mean square (RMS) deviation from the set-point. It is magnetically shielded with two insulated layers of μ -metal. A housing around the cell mount with small openings for the laser beam reduces air flow.

The reference laser frequency is locked to the F=3 to F'=4 hyperfine transition in ⁸⁵Rb which exhibits the error signal with the steepest slope in our setup. To study the laser frequency instability and systematic shifts, part of the laser power is overlapped with the output of a stabilized optical frequency comb and a beat note is recorded on a high bandwidth photo diode.

Performance of the reference laser

Since the rubidium vapor is enclosed in a fixed volume, any temperature change translates directly into a pressure change. In an atomic vapor, pressure not only broadens the transition lines, but also shifts them in energy [44]. By changing the set-point of the temperature stabilization while observing the beat frequency over time on an electronic counter, a temperature sensitivity of ~ 100 kHz/K is measured for the here used transition. Our stabilization is restricting temperature fluctuations to ~ 10 mK, leading to a frequency instability on the few-kHz level.

The differential magnetic field shift of the hyperfine levels used for laser stabilization is 2.3 MHz/mT [40]. With typical magnetic field fluctuations on the order of 10^{-2} mT and shielding as described above, magnetic field shifts are negligible on the kHz level.

While for a perfectly symmetric error signal only the slope of the signal varies with laser power, for an asymmetric error signal its zero-crossing shifts in frequency relative to the atomic transition. An asymmetry arises from RAM at the EOM modulation frequency and thus depends on alignment of the setup and radio frequency (rf) power used to drive the EOM [42]. In order to study the influence of laser power fluctuations on the laser frequency we vary the optical power going into the MTS setup while recording both laser power and beat frequency. For relative changes below 10 % the laser frequency responds to a good approximation linearly to a change in laser power (see Fig. 3). When operating at the optimum power level, a sensitivity for absolute laser frequency shift per unit optical power shift can be extracted. With the parameters used in our measurements, we obtain a sensitivity of 91 kHz/mW. We observe laser power fluctuations up to $\pm 8\%$ or 0.35 mW. The resulting fluctuations in the zero-crossing are the main source of residual frequency fluctuations in the reference laser. This effect could be suppressed by an active laser power stabilization.

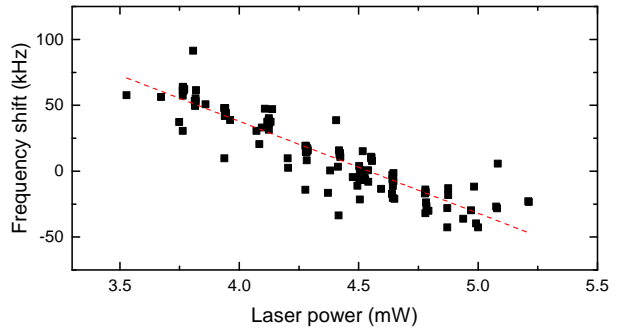


Fig. 3 Frequency shift of the reference laser relative to optimal laser power recorded versus laser power in the modulation transfer spectroscopy setup. For small laser power deviations a linear dependence of 91 kHz per mW laser power deviation is extracted (dashed line).

The spectral distribution of the beat note between the reference laser and the frequency comb, which is stabilized to an optical reference, is recorded on a spectrum analyzer. The linewidth of the stabilized reference laser is estimated by fitting a Gaussian profile to the spectral distribution. This signal is a convolution of the ~ 100 kHz broad comb tooth with the reference laser line. An upper bound for the linewidth of 400 kHz is determined for the reference laser.

The long-term frequency stability is evaluated by several comparisons against an active hydrogen maser frequency standard with the help of the frequency comb

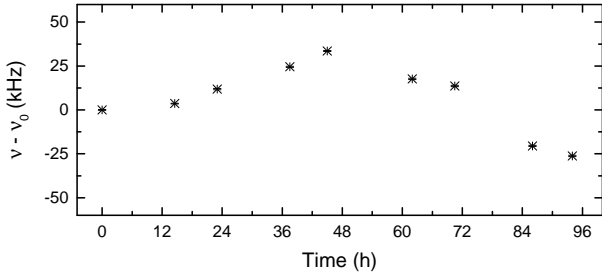


Fig. 4 Reference laser frequency measurements relative to the absolute frequency $\nu_0 = 384.229\,240\,061$ THz of the first data point. Each data point is averaged over 30 seconds. The offset of 1.6 MHz from the literature value [40] arises from a finite magnetic field, a pressure shift and the asymmetric error signal.

over the course of 4 days. Fig. 4 shows for each measurement the frequency deviation of the reference laser relative to the first measurement. In a time interval of 4 days the frequency is well stabilized within 100 kHz, the RMS deviation being 20 kHz. At a wavelength of 780 nm this corresponds to a fractional instability of the absolute laser frequency of 5×10^{-11} .

2.2 Transfer lock

A schematic overview of the cavity transfer lock is shown in the upper right-hand box in Fig. 1. To sustain a cavity transfer lock bridging 100 nm in the optical/infrared range, care has to be taken to suppress differential dispersion inside the cavity arising from temperature, pressure and relative humidity fluctuations in the air. To that end, evacuated cavities are commonly employed [45–47].

A 25 mm diameter Invar rod with a through hole, and a ring piezo at one end of the rod make up a 100 mm long cavity spacer. Two curved mirrors with $R = 250$ mm are glued to both ends of the spacer, yielding a symmetric cavity with a free spectral range of about 1500 MHz. The length of the cavity was chosen such that higher order modes do not coincide with PDH modulation signals. Otherwise, beam pointing fluctuations change the optical power in these modes distorting the main signal, as each cavity mode creates an error signal with a width of twice the modulation frequency [48].

The broadband HR coating of the cavity mirrors reflects more than 99 % of the light in the wavelength range between 775 … 890 nm. For our employed wavelengths of 780 and 882 nm we measure a finesse of about 300 and 400, respectively. The spacer is placed in a small vacuum chamber with vibration insulated mounting. An attached 21/s ion pump maintains a vacuum of $\sim 10^{-8}$ mbar.

The electronic sideband locking technique [49] based on PDH stabilization is used to stabilize the length of the cavity to the 780 nm reference laser. The basic idea is to create a sideband with a tunable offset to the carrier

laser frequency. This sideband itself exhibits phase modulation sidebands for PDH stabilization. If the variable offset spans a range of half an FSR, then the cavity can be locked to one or the other of the offset sidebands for any desired spectroscopy laser frequency. The electronic signal necessary to create the above mentioned sidebands is a phase modulated rf signal with variable carrier frequency up to FSR/2, in our case 750 MHz. To create the phase modulated rf signal (see upper right box in Fig. 1), a VCO (Mini-Circuits ZX95-800C) at 798 … 803 MHz is locked to a fixed frequency PLL at 800 MHz, referenced to a maser-stabilized 10 MHz source. The stabilized VCO frequency is phase modulated with about 9.3 MHz. Mixing the VCO output with a signal generator at 810 … 1600 MHz creates sum and difference frequencies from 1610 … 2400 MHz and 10 … 800 MHz, respectively. A low-pass filter with a cutoff at 800 MHz removes the sum frequency. This signal is applied to a fiber-coupled EOM (Photline NIR-MPX800-LN-05) with an rf bandwidth of 5 GHz.

Fig. 5 shows a trace of the error signal obtained in our setup together with the corresponding cavity transmission photo diode signal. We can vary the carrier rf ω_{var} between 10 … 800 MHz, while ω_{PDH} is fixed to ~ 9.3 MHz. Exploiting the opposite sign of the slopes for the error signals at $\pm\omega_{\text{var}}$ from the carrier, one free spectral range of 1500 MHz is covered with this technique.

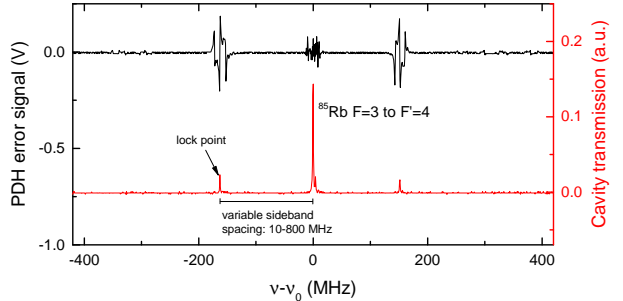


Fig. 5 Photo diode signal of the transfer cavity transmission around the transition frequency ν_0 for $F=3$ to $F'=4$ in ${}^{85}\text{Rb}$ (red) and corresponding PDH error signal (black). In the photo diode trace, due to scaling, only the sidebands at ω_{var} can be seen, the sidebands at ω_{PDH} can be inferred from the error signal. The slopes of the error signals at $\pm\omega_{\text{var}}$ have opposite signs.

The feedback loop stabilizing the cavity length to the reference laser is electronically bandwidth limited to 150 Hz. Therefore, frequency noise on the reference laser with Fourier frequencies above 150 Hz is filtered out and does not affect the cavity length. This allows us to transfer the mean frequency stability of the reference laser without being limited by its high-frequency noise.

2.3 Spectroscopy laser

A Ti:Sapphire ring laser (TekhnoScan TIS-SF-07) is used as a light source at 882 nm. It is optically pumped with 10 watts at 532 nm by a diode pumped solid state laser (Verdi G10). The output power of ~ 500 mW is split in 20 mW towards the transfer cavity and the remaining power towards a second harmonic generation stage.

The beam towards the transfer cavity is phase modulated at 91 MHz in a resonant-circuit EOM (TimeBase EOM-320IR). A PDH setup generates an error signal from the cavity-reflected beam. The signal is modified by a PI controller which feeds back to two feedback channels acting upon different piezo actuators inside the resonator. The fast channel expects a high voltage input and is directly connected to a fast piezo actuator with low stroke. A small mirror mounted on the actuator serves to compensate high-frequency fluctuations with low modulation index. The resonance frequency of this feedback channel is above 50 kHz. The other channel amplifies the signal from the PI controller and drives three large piezo ring actuators with mounted cavity mirrors. This channel compensates low-frequency fluctuations up to several 100 Hz with high amplitude.

Performance of the spectroscopy laser

The linewidth of the locked spectroscopy laser is characterized by comparison with an ultra-stable laser at 1542 nm locked to a high-finesse passive cavity obtaining a linewidth of ~ 1 Hz. For both lasers a beat note with the frequency comb is recorded using a 200 MS/s digital oscilloscope which digitizes 10^7 data points of three traces within 50 ms. With the simultaneously recorded carrier envelope offset of the frequency comb the relative phase shift between our spectroscopy laser and the ultra-stable laser is calculated, suppressing the noise of the frequency comb [50]. From this information, the frequency of the spectroscopy laser for each data point and the frequency noise spectral density is extracted. Within the 50 ms time interval the ultra-stable laser is, relative to the spectroscopy laser's spectral distribution, assumed to be a δ -function in frequency space. The inset of Fig. 6 shows the distribution of the spectroscopy laser's frequency fluctuations around the mean value. As the spectral distribution shows no Gaussian shape, an estimate for the linewidth is inferred from the frequency noise spectral density. In Ref. [51] a method is presented to extract a laser linewidth from arbitrary spectral noise distributions. The frequency noise spectrum can be divided into two regions. One with a high noise level compared to the Fourier frequency, thus exerting a modulation index $\beta > 1$, and one with a low noise level compared to the Fourier frequency, yielding a low modulation index. The first region contributes to the linewidth, while the latter mostly affects the wings of the laser line. These regions

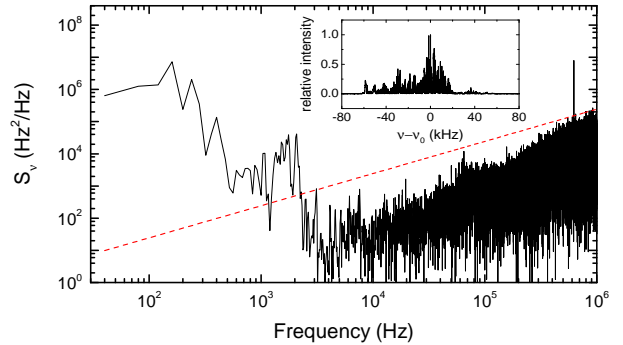


Fig. 6 Frequency noise spectral density S_ν of the spectroscopy laser in transfer locked state (solid line). The β -separation line (dashed line) separates the areas of high and low modulation index. The inset shows a 50 ms snapshot of the laser frequency compared to another laser with ~ 1 Hz linewidth.

are separated by the so called β -separation line. The full width at half maximum (FWHM) of the laser linewidth is extracted by integrating the frequency noise spectral density up to the Fourier frequency where it intersects the β -separation line, which in our case is about 2.2 kHz, see Fig. 6. Applying this method we derive a FWHM of 55 kHz. The RMS deviation of the laser frequency distribution in the inset of Fig. 6 is 23 kHz.

We characterize our stabilization by comparing the power spectral densities (PSD) of the in-loop error signal for two cases: a tight lock with optimized parameters and a loose lock where the stabilization is just sufficient to keep the laser frequency on the central slope of the PDH error signal. That way, we obtain a nearly linear voltage response for frequency fluctuations. Fig. 7 shows PSD spectra up to 100 kHz recorded with a fast Fourier transform device. It can be seen that the feedback loop suppresses noise within a bandwidth of about 18 kHz.

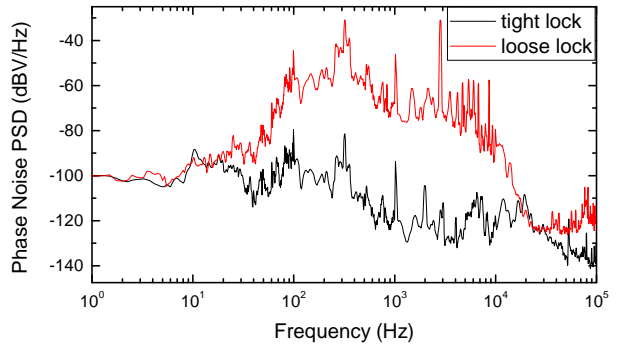


Fig. 7 Phase noise power spectral density of the Ti:Sapphire laser in tight lock (black) and loose lock (red). A noise suppression of up to 50 dB is established by the cavity lock. We infer a feedback bandwidth of around 18 kHz for the fast feedback channel from the crossing point of the two curves. The difference in PSD above 18 kHz between both curves arises from a nonlinear response of the in-loop error signal for high-frequency deviations exceeding the PDH slope.

With the transfer lock engaged, the frequency instability of the spectroscopy laser is measured the same way as before for the reference laser. The wavelength of the spectroscopy laser is tuned to 871 nm where an output port of a frequency comb is available. The beat frequency between spectroscopy laser and frequency comb is monitored over several days. Fig. 8 (a) shows a fre-

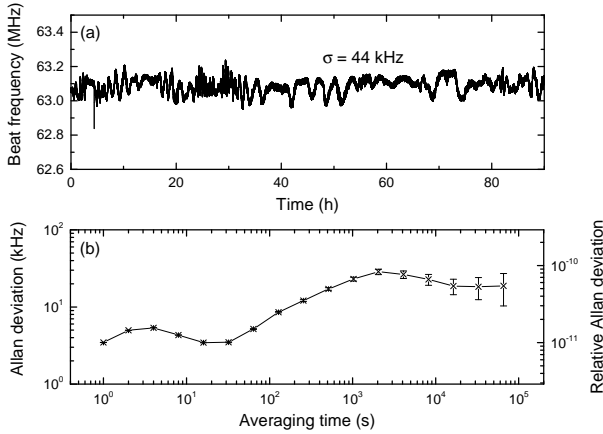


Fig. 8 (a) Beat frequency of the transfer locked spectroscopy laser with a frequency comb at 871 nm. (b) Absolute and relative overlapping Allan deviation of the transfer locked spectroscopy laser up to averaging times of 6.5×10^4 s.

quency trace taken over 90 hours. A linear fit on the data suggests a frequency drift of (0.28 ± 0.30) kHz/h. The RMS frequency deviation is 44 kHz. More information on the stability can be extracted from the Allan deviation in Fig. 8 (b). We achieve a frequency instability below 10^{-10} for averaging times up to 18 h. At that point the Allan deviation flattens out, indicating no linear drift on this time scale.

We expect that the lower limit in Allan deviation is given by the instability of the reference laser. The stability of the spectroscopy laser is further deteriorated by offset fluctuations in the PDH error signals due to residual amplitude modulation.

3 Conclusion

We have presented a laser setup that combines tunability over 100 nm in the infrared with frequency fluctuations below 50 kHz over several days. The fast linewidth is on the order of 50 kHz. These values were verified by measurements with a referenced optical frequency comb. We show that the spectral impurity of the reference laser does not limit the spectroscopy laser linewidth due to the frequency noise low-pass filtering effect of the transfer cavity. The transfer locking technique demonstrated here can be extended to cover a broad range of wavelengths in the optical and infrared, limited only by the cavity mirror coating.

Current limitations in our frequency stabilization setup arise mainly from the reference laser. A simple improvement would be a laser power stabilization of the reference laser and a temperature stabilization of the EOM used for the modulation transfer spectroscopy to reduce time-varying RAM. Furthermore, an improved temperature stabilization of the rubidium vapor cell would further improve the stability of the reference. To narrow the short term linewidth of the spectroscopy laser, a higher feedback bandwidth is necessary. An intracavity EOM or external AOM [52,53] could be used for this purpose. Additionally, the cavity mirror coating should then be tailored in such a way, that the finesse is substantially higher for the spectroscopy laser while keeping a value on the order of 100 for the reference laser.

With this setup we anticipate to resolve the line of the fine structure transition $1s^2 2s^2 2p\ ^2P_{1/2} - \ ^2P_{3/2}$ at 441 nm in Coulomb-crystallized Ar^{13+} ions in a Paul trap to within 100 kHz.

Acknowledgments

We acknowledge support from DFG through QUEST. I.D.L. acknowledges a fellowship from the Alexander von Humboldt Foundation. This work was funded by PTB.

References

1. A. D. Ludlow, M. M. Boyd, J. Ye, E. Peik, and P. O. Schmidt, Rev. Mod. Phys. **87**, 637–701 (2015).
2. N. Poli, C. W. Oates, P. Gill, and G. M. Tino, Riv. Nuovo Cimento **36**, 555–624 (2013).
3. C. W. Chou, D. B. Hume, J. C. J. Koelemeij, D. J. Wineland, and T. Rosenband, Phys. Rev. Lett. **104**, 070802 (2010).
4. T. L. Nicholson, S. L. Campbell, R. B. Hutson, G. E. Marti, B. J. Bloom, R. L. McNally, W. Zhang, M. D. Barrett, M. S. Safronova, G. F. Strouse, W. L. Tew, and J. Ye, Nat. Commun. **6**, 6896 (2015).
5. R. M. Godun, P. B. R. Nisbet-Jones, J. M. Jones, S. A. King, L. A. M. Johnson, H. S. Margolis, K. Szymaniec, S. N. Lea, K. Bongs, and P. Gill, Phys. Rev. Lett. **113**, 210801 (2014).
6. N. Huntemann, B. Lipphardt, C. Tamm, V. Gerginov, S. Weyers, and E. Peik, Phys. Rev. Lett. **113**, 210802 (2014).
7. A. Shelkovnikov, R. J. Butcher, C. Chardonnet, and A. Amy-Klein, Phys. Rev. Lett. **100**, 150801 (2008).
8. J. Berengut, V. Dzuba, and V. Flambaum, Phys. Rev. Lett. **105**, 120801 (2010).
9. J. Berengut, V. Dzuba, V. Flambaum, and A. Ong, Phys. Rev. A **86**, 022517 (2012).
10. M. Safronova, V. Dzuba, V. Flambaum, U. Safronova, S. Porsev, and M. Kozlov, Phys. Rev. Lett. **113**, 030801 (2014).
11. V. Mäckel, R. Klawitter, G. Brenner, J. C. López-Urrutia, and J. Ullrich, Phys. Rev. Lett. **107**, 143002 (2011).

12. L. Schmöger, O. O. Versolato, M. Schwarz, M. Kohnen, A. Windberger, B. Piest, S. Feuchtenbeiner, J. Pedregosa-Gutierrez, T. Leopold, P. Micke, A. K. Hansen, T. M. Baumann, M. Drewsen, J. Ullrich, P. O. Schmidt, and J. R. Crespo López-Urrutia, *Science* **347**, 1233 (2015).
13. B. C. Young, F. C. Cruz, W. M. Itano, and J. C. Bergquist, *Phys. Rev. Lett.* **82**, 3799–3802 (1999).
14. T. Kessler, C. Hagemann, C. Grebing, T. Legero, U. Sterr, F. Riehle, M. J. Martin, L. Chen, and J. Ye, *Nature Photon.* **6**, 687–692 (2012).
15. S. Häfner, S. Falke, C. Grebing, S. Vogt, T. Legero, M. Merimaa, C. Lisdat, and U. Sterr, *Opt. Lett.* **40**, 2112 (2015).
16. E. Benkler, F. Rohde, and H. R. Telle, *Opt. Lett.* **38**, 555–557 (2013).
17. H. Inaba, K. Hosaka, M. Yasuda, Y. Nakajima, K. Iwakuni, D. Akamatsu, S. Okubo, T. Kohno, A. Onae, and F.-L. Hong, *Opt. Express* **21**, 7891–7896 (2013).
18. F. Rohde, E. Benkler, T. Puppe, R. Unterreitmayer, A. Zach, and H. R. Telle, *Opt. Lett.* **39**, 4080–4083 (2014).
19. D. Nicolodi, B. Argence, W. Zhang, R. Le Targat, G. Santarelli, and Y. Le Coq, *Nature Photon.* **8**, 219–223 (2014).
20. N. Scharnhorst, J. B. Wübbena, S. Hannig, K. Jakobsen, J. Kramer, I. D. Leroux, and P. O. Schmidt, *Opt. Express* **23**, 19771–19776 (2015).
21. C. Wieman and T. W. Hänsch, *Phys. Rev. Lett.* **36**, 1170–1173 (1976).
22. K. L. Corwin, Z.-T. Lu, C. F. Hand, R. J. Epstein, and C. E. Wieman, *Appl. Opt.* **37**, 3295–3298 (1998).
23. J. Ye, L.-S. Ma, and J. L. Hall, *JOSA B* **15**, 6–15 (1998).
24. J. H. Shirley, *Opt. Lett.* **7**, 537 (1982).
25. G. C. Bjorklund, M. D. Levenson, W. Lenth, and C. Ortiz, *Appl. Phys. B* **32**, 145–152 (1983).
26. D. J. McCarron, S. A. King, and S. L. Cornish, *Meas. Sci. Technol.* **19**, 105601 (2008).
27. E. Riedle, S. H. Ashworth, J. T. Farrell Jr., and D. J. Nesbitt, *Rev. Sci. Instrum.* **65**, 42 (1994).
28. S. Vogt, C. Lisdat, T. Legero, U. Sterr, I. Ernsting, A. Neovsky, and S. Schiller, *Appl. Phys. B* **104**, 741–745 (2011).
29. Q.-F. Chen, A. Neovsky, M. Cardace, S. Schiller, T. Legero, S. Häfner, A. Uhde, and U. Sterr, *Rev. Sci. Instrum.* **85**, 113107 (2014).
30. D. R. Leibrandt, M. J. Thorpe, J. C. Bergquist, and T. Rosenband, *Opt. Express* **19**, 10278–10286 (2011).
31. D. R. Leibrandt, M. J. Thorpe, M. Notcutt, R. E. Drullinger, T. Rosenband, and J. C. Bergquist, *Opt. Express* **19**, 3471–3482 (2011).
32. P. Dubé, A. Madej, J. Bernard, L. Marmet, and A. Shiner, *Appl. Phys. B* **95**, 43–54 (2009).
33. P. Bohlouli-Zanjani, K. Afrousheh, and J. D. D. Martin, *Rev. Sci. Instrum.* **77**, 093105 (2006).
34. S. Uetake, K. Matsubara, H. Ito, K. Hayasaka, and M. Hosokawa, *Appl. Phys. B* **97**, 413 (2009).
35. F. Rohde, M. Almendros, C. Schuck, J. Huwer, M. Henrich, and J. Eschner, *J. Phys. B* **43**, 115401 (2010).
36. S. Albrecht, S. Altenburg, C. Siegel, N. Herschbach, and G. Birk, *Appl. Phys. B* **107**, 1069–1074 (2012).
37. Y. Yin, Y. Xia, X. Li, X. Yang, S. Xu, and J. Yin, *Appl. Phys. Express* **8**, 092701 (2015).
38. E. M. Bridge, N. C. Keegan, A. D. Bounds, D. Boddy, D. P. Sadler, and M. P. A. Jones, *Opt. Express* **24**, 2281–2292 (2016).
39. E. D. Black, *Am. J. Phys.* **69**, 79 (2001).
40. D. A. Steck, *Rubidium 85 D Line Data (revision 2.1.4, 2010)*.
41. D. A. Steck, *Rubidium 87 D Line Data* (2001).
42. E. Jaatinen and J. M. Chartier, *Metrologia* **35**, 75 (1998).
43. Y. N. M. de Escobar, S. P. Álvarez, S. Coop, T. Vanderbruggen, K. T. Kaczmarek, and M. W. Mitchell, *Opt. Lett.* **40**, 4731 (2015).
44. M. Ardit and T. R. Carver, *Phys. Rev.* **124**, 800 (1961).
45. J. Hough, D. Hils, M. D. Rayman, L.-S. Ma, L. Hollberg, and J. L. Hall, *Appl. Phys. B* **33**, 179 (1984).
46. J. Helmcke, J. J. Snyder, A. Morinaga, F. Mensing, and M. Gläser, *Appl. Phys. B* **43**, 85 (1987).
47. W. Z. Zhao, J. E. Simsarian, L. A. Orozco, and G. D. Sprouse, *Rev. Sci. Instrum.* **69**, 3737 (1998).
48. S. Amairi, T. Legero, T. Kessler, U. Sterr, J. B. Wübbena, O. Mandel, and P. O. Schmidt, *Appl. Phys. B* **113**, 233–242 (2013).
49. J. Thorpe, K. Numata, and J. Livas, *Opt. Express* **16**, 15980–15990 (2008).
50. H. R. Telle, B. Lipphardt, and J. Stenger, *Appl. Phys. B* **74**, 1 (2002).
51. G. Di Domenico, S. Schilt, and P. Thomann, *Appl. Opt.* **49**, 4801 (2010).
52. D. Haubrich and R. Wynands, *Opt. Commun.* **123**, 558–562 (1996).
53. T. L. Boyd and H. Kimble, *Opt. Lett.* **16**, 808–810 (1991).